Purpose of the visit

During my short visit of the Theoretical Physics Department at Loughborough University I continued working on the the subject

Two particle element for magnetic memory

together with Prof. Kusmartsev and his PHD student Mike Forrester. The results are very encouraging and promising. We made essential progress in the analytical and numerical derivation of phase diagrams, the calculation of the corresponding hysteresis curves as well as the energy landscapes and their physical interpretation.

Short description about the project

We propose a stack of two isolated diskshape particles as an element for magnetic memory storage. The tunneling across the device depends on the magnetic arrangement of the magnetic moments of the two magnetic particles and is appreciably higher when the magnetic moments are aligned parallel to one another. Such a device is characterised by a few stable states separated by large barriers. The switching between different states may be induced by an applied spin-polarised current or magnetic field. We present a complete theoretical study of the magnetic phase diagrams as a function of the field for arbitrary strength of the anisotropy and arbitrary directions of the external magnetic field. We classify all possible magnetic hysteresis loops. We further discuss the stability of the information stored and determine the critical magnetic switching fields.

For completeness I include the current version of our paper.

Future collaboration with the host institution

The long lasting collaboration Vienna-Loughborough with Prof. Kusmartsev is intended to be continued in the future. Considering that the subject is of high actual interest, especially in the range of technical applications, we plan to do further joint work in the field of magnetic nanoparticles and also in the field of arrays of Josephson junctions.

Two particle element for magnetic memory

D. M. Forrester,, Karl E. Kürten*,, and F. V. Kusmartsev
Department of Physics, Loughborough University, LE11 3TU, UK and
**Institute for Experimental Physics, University of Vienna, 5, Boltzmanngasse, A-1090 Vienna, Austria*
(Dated: January 25, 2007)

We propose to use a stack of two or more isolated disk-shaped particles as an element for magnetic memory, i.e. as a magnetic tunnel junction. Such a junction is characterised by a few stable states separated by large energy barriers. The switching between the states may be induced by applying a spin polarised current or a magnetic field. We have described the behaviour of the stable states and energies of the stack in magnetic fields. In addition, we have described the magnetisations as well as all possible types of hysteresis loops which such an element may have. We discuss the stability of the information stored in the element and determine a critical magnetic field at which the switching of the element arises.

PACS numbers:

INTRODUCTION

On one hand the emerging technology known as spintronics is going to make a step towards the use of spin degrees of freedom. On the other the magnetic memory structures have a tendency to be made of smaller and smaller elements. With the ever decreasing scales of these elements comes the necessity to find greater understanding of their magnetisation properties, their responses to applied fields and their hysteretic characteristics. One form of magnetic memory is magnetoresistive random access memory (MRAM) that uses the magnetic tunnel junction (MTJ) to store information[9]. Within this element the MTJ stack consists of two ferromagnetic layers separated by a thin dielectric barrier. Usually a magnetic polarization of one layer is fixed, while the other is used for information storage. MRAM stores data by utilizing the magnetic polarity of a ferromagnetic layer[10]. The reading of information is performed by measuring the current, which is determined by the rate of electron quantum tunnelling through the MTJ stack. This is affected by the mutual polarity of the layers[11–13]. In other terms the MTJ resistance is measured across the stack to determine the cell state. The free layer polarization is changeable: thus parallel or anti-parallel magnetic moments give low or high resistances which can be interpreted as "0" or "1." When the free and fixed layers have the same orientation the resistance is lower.

The MRAM will be a non-volatile, power-saving, high-speed memory in the future[15]. In MRAM, thermal agitation combined with either digit or word write line disturbances limit the operational field margin. This causes unexpected switching and affects the stability of the memory states. The development of new structures is required to increase the operational field margin for effective reading and writing in MRAM[16]. In most of the proposals, from Goto's model to the tri-layer model, the energy barriers become lower with an increase of the applied magnetic field. Thermal agitation combined with field disturbances in the easy direction may cause unexpected switches.

The memory consists of an array of the MRAM cells. Increasing the density of an MRAM array is only possible by decreasing the size of the MTJ. However with small sizes there are issues such as thermal instability of the cell states[21]. As size decreases barrier energy drops as well and begins the onset of instability. The critical magnetic field cannot simply be raised because this also generates an increased current flow. In some proposals one uses the thermal heat itself to help select the cell for writing[18–20]. As a material approaches its Curie point, Hc drops, so that less current is needed to write the information[17]. At cooler temperatures the energy potential well can be deeper. This will lead to increased stability of the MRAM cell states and the stored information. We have to avoid thermal instabilities by increasing barrier heights. In some proposals the free layer is in fact a Synthetic Antiferromagnetic tri-layer stack (SAF)[18–20]. The magnetic moments of the top and bottom layers are nearly balanced. The direction of magnetization of the ferromagnetic (FM) sense layer with respect to the pinned FM layer determines the resistance state of the bit. The direction of the top FM layer and the sense FM layer are set by Savtchenko switching. Savtchenko switching is named after the late Leonid Savtchenko at Motorola. Savtchenko switching is a method to toggle bit between high and low resistance states. The SAF rotates its magnetic axis perpendicular to the applied field. The bit is oriented at 45 degrees to the write lines. The 45 degree bits result in higher memory storage densities.

We propose to use small magnetic disk-shaped particles to build up a MTJ. A most simple construction of MTJ can consist of two monodomain ferromagnets separated by an insulator or normal metal. The monodomain nanodots can be made of NiZn with a diameter of about d 40 nm or supermalloy with a diameter d 100nm and thickness h 10nm. The magnetism at small length scales has been a rapidly growing area of physics. Small magnetic particles and

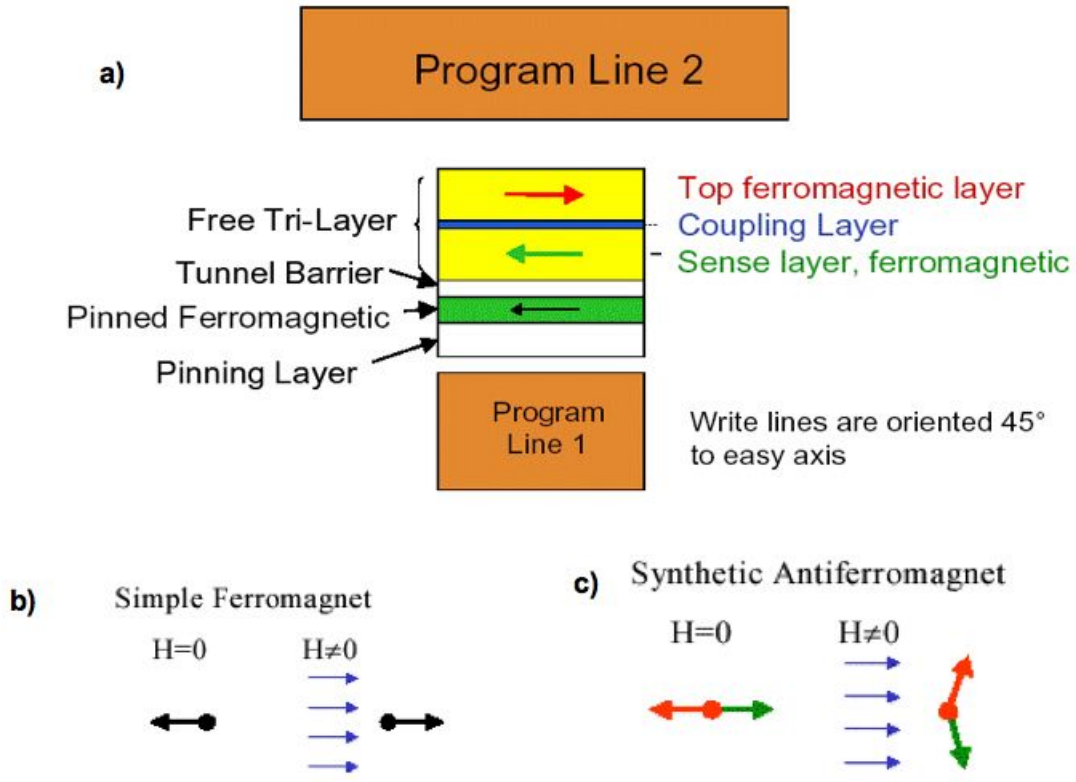

FIG. 1: a) Schematic structure of the work of the Magnetoresistive Access Memory (MRAM) cell consisting of magnetic tunnel junction formed by two ferromagnetic and one insulating layers From the top and bottom from the memory cell there are to programm lines which responsible for reading and writing information into the cell.

artificial thin-film structures that are based on ferromagnetic or anti-ferromagnetic layers separated by non-magnetic spacers are the basic structural elements for an enormous scope of technical applications. Data storage and magnetic sensing are just some of the areas in everyday life where they find uses[18**?** –20].

The formation of a MTJ through the giant magnetoresistant (GMR) effect in anti-ferromagnetically coupled multi-layers is in a heart of many specific applications [1, 2]. On the other hand, nanomagnets can provide the basis for experimental systems used to study fundamental phenomena in spintronics. Because of the hierarchy of competing interactions these many particle systems display rather rich and interesting collective behaviour not found in bulk crystalline magnets. Networks of elementary interacting small magnetic particles, smaller than the bulk domain size, are potential future candidates for MRAM to store and to propagate information. The states are signalled by the magnetization direction of single-domain magnetic particles coupled to their nearest neighbours through magnetostatic interactions. New memory may consist of a network or a one-dimensional chain of circular or elliptic pairs of disk shaped monodomain particles. These could form MTJs made from a commonly used magnetic supermalloy on a single-crystal silicon substrate. Cowburn et al. have shown experimentally that circular nanomagnets made from supermalloy behave like single domains if their diameter is less than 100nm and their thickness is not more than 10nm [3]

NUMERICAL MODELLING

In a ferromagnetic material the atomic dipole moments are coupled strongly and tend to align themselves in parallel. This produces a spontaneous magnetisation in materials of this classification. As Weiss [] postulated, a material consists of many small regions which are each spontaneously magnetised. These regions are called domains. The magnetic moment of the ferromagnet as a whole is dependent upon the contingent of domains in the specimen

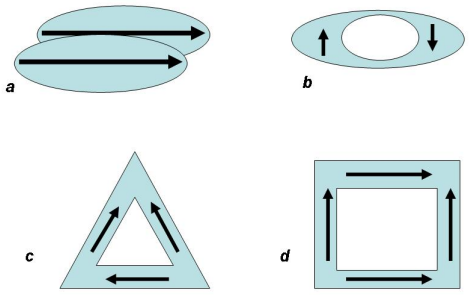

FIG. 2: Different elements for magnetic memory.

and as such can be taken as a sum of their moments. Generally the direction of each domain does not necessarily align and the juxtaposition of individual domain moments may sum to an overall value of zero for certain configurations. However, the application of a magnetic field adjusts the domain orientations and gives a net magnetisation. Usually a specimen will consist of many domains, but as the size of the sample becomes smaller and smaller the propensity to produce single domain particles increases. These single domain particles also emerge when a specimen is magnetised to a level of saturation under the influence of a very large external field. Here bodies of nanometre scale dimensions are examined with a view to highlighting the magnetic energies of such systems. Each particle is magnetised along the length of its longest axis and geometry dictates that shape anisotropy has a major bearing upon the internal properties. The particles investigated have the geometries of elliptical cylinders with a-semiaxis lengths of 70nm, b-semiaxis lengths of 35nm, and thicknesses of 30nm. For a body of any particular shape and magnetisation $\mathbf{M}$, the energy of interaction in an applied field $\mathbf{H}_0$ is

$$E_H = -\mu_0 \int (\mathbf{M} \cdot \mathbf{H}_0)\, dV \tag{1}$$

The magnetostatic energy is given as,

$$E_m = \frac{\mu_0}{2} \int\limits_{All\ Space} H_m^2 dV = -\frac{\mu_0}{2} \int\limits_{Body} \mathbf{H}_m \cdot \mathbf{M} dV \tag{2}$$

This means that the internal energy of a body is equal to the negative of its counterpart in the external space (as the magnetisation is zero everywhere except inside the particle). With increasing applied magnetic field strength the distribution of the magnetic flux density for two single domain iron particles is shown in Figure 2. As the field increases the magnetic flux density of the particle with magnetization in the direction of the field is enhanced whilst the one originally directed into the field will undergo rotation until its magnetisation becomes parallel with the direction of the field. In the particle where the field is directed opposite to the magnetisation direction, shape anisotropy will try to maintain the initial orientation. For small magnetic fields the shape effect has the greater influence and so dominates. However, as the field is increased the shapes control waivers and at a critical level of applied field the magnetisation experiences a complete flip to align itself with its competitor.

Taking the perspective that logic operations may be conducted by considering spins of plus and minus one, indicated in Figure 3 by the positively and negatively directed arrows, the four system states within such a scheme are shown in the aforementioned diagram. There exists an exact degeneracy of the antiferromagnetically ordered states, as is seen in the lowest ground state energy of the diagram. There are a further two clear energy contours that exist for pairs of particles that have the same vector alignment of their magnetisations. With no applied magnetic field there are two points of magnetic energy and it is not until the field is switched on that the branching from the zero field state occurs in the upper level. The interaction between the particles can be described by $J_0 S_i S_{i+1}$ where S is the direction of the spin and J_0 is the interaction energy. From Figure 4 the value of J_0 is around $4eV$.

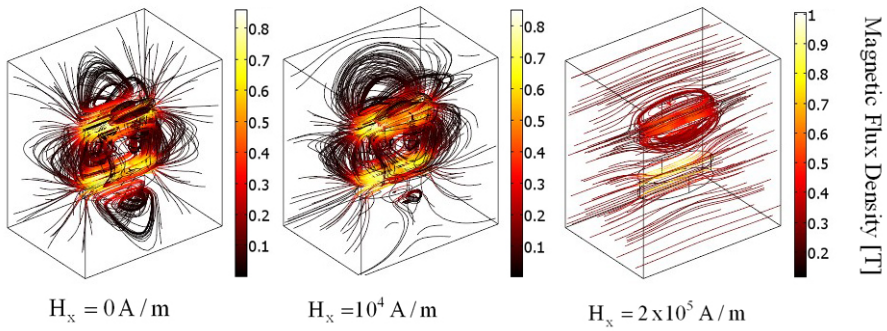

FIG. 3: The magnetic flux density distribution **B** as a function of magnetic field strength **H**. The field is applied along the x-direction with 0, 10^4 and 2 x 10^5 A/m. The top particle is initially magnetised in the direction opposite to the field, whereas the bottom one is aligned with it.

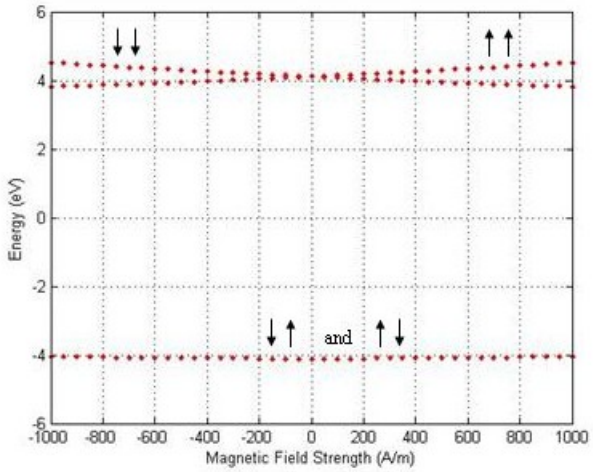

FIG. 4: The magnetic energy as a function of magnetic field strength. The arrows next to the curves are indicative of the direction of the magnetisations in each particle in the system, i.e. there are four system orientations represented here. The difference in the energies of the ground state and the excited level at a field strength equal to zero is about 8eV giving a value of J_0 of around $4eV$.

2. THE MODEL SYSTEM

Consider a thin film sandwich structure with two ferromagnetic layers separated by an insulating layer. Depending on the thickness of the spacer the two layers can be ferromagnetically or antiferromagnetically coupled. We start with the Hamiltonian of the classic anisotropic Dirac-Heisenberg model

$$H = -J \sum_{<i,j>} \mathbf{S}_i \cdot \mathbf{S}_j + K \sum_{i=1}^{N} (\mathbf{S_i} \cdot \mathbf{e}_y)^2 - \mathbf{H} \cdot \sum_{i=1}^{N} \mathbf{S}_i \tag{1}$$

where the spin operators are substituted by the unit vectors S_i corresponding to the spin on site i. H is the uniform magnetic field applied in a direction of the angle β with respect to the easy axis. The quantity $K > 0$ specifies the strength of the uniaxial unisotropy, while the quantity J describes the strength of the nearest-neighbor exchange interaction. We remark that the dipole-dipole interaction inside the particles is neclected, since for small spherical particles this energy contribution is small compared with the contribution to the exchange interactions. The same argument holds for the shape anisotropy such that the anisotropy contribution mainly stems from surface effects. The locally energy minima of the system whose stabilities are crucial for hysteresis effects can be determined from the

integration of the Landau Lifshitz Gilbert equation [4]

$$\dot{\mathbf{S}}_\mathbf{i} = \mathbf{S}_\mathbf{i} \times \frac{\partial H}{\partial \mathbf{S}_\mathbf{i}} - \alpha \mathbf{S}_\mathbf{i} \times (\mathbf{S}_\mathbf{i} \times \frac{\partial H}{\partial \mathbf{S}_\mathbf{i}}) \tag{2}$$

with the relaxation parameter α, which is often known from experimental studies. Assuming that within each layer all magnetic moments are ferromagnetically aligned but with an orientation that differs from layer to layer, we consider the particles as elementary mono-domain units which take the shape of very flat spheres. Under these assumptions the preferential orientations of the magnetizations are in-plane such that we can reduce our problem to the study of one-dimensional chains of small magnetic particles. Introducing planar polar coordinates $\mathbf{S}_i = (\cos(\phi_i), \sin(\phi_i))$, where the magnetization direction of particle i is described by the variable ϕ_i. the total energy of the system is given by the two-particle Hamiltonian

$$H = -2J\cos(\phi_1 - \phi_2) + \frac{K}{2}\left(\sin^2(\phi_1) + \sin^2(\phi_2)\right) - H\left(\cos(\phi_1 - \beta) + \cos(\phi_2 - \beta)\right) \tag{3}$$

The quantity β specifies the angle of the external field with the easy axis, The dynamical behaviour of the particles is governed by three competing energy terms, which can give rise to multistability and coexistence of various physical phases. The first term defines the exchange energy, specified by nearest-neighbour interactions, while the next two terms are due to the anisotropy. The last two terms specify the Zeeman energy. Since H and K can be scaled by J we can choose $|J| = 1$. The set of Landau Lifshitz Gilbert equations collapses to the two coupled ordinary differential equations

$$\dot{\phi}_1 = -\alpha \frac{\partial H}{\partial \phi_1} \qquad \text{and} \qquad \dot{\phi}_2 = -\alpha \frac{\partial H}{\partial \phi_2} \tag{4}$$

Discretization of Eqs. (4) leads to a gradient descent procedure as commonly practised. Here, depending on the initial condition, the system relaxes to the "closest" local or global minimum. According to the variational principle, the necessary conditions for the existence of a local minimum of the Hamiltonian are the force equilibrium equations

$$\frac{\partial \mathbf{E}}{\partial \phi_1} = 2J\sin(\phi_1 - \phi_2) + H\ \sin\ (\phi_1 - \beta) + K\ \sin(\phi_1)\cos(\phi_1) = 0 \tag{5}$$

and

$$\frac{\partial \mathbf{E}}{\partial \phi_2} = 2J\sin(\phi_2 - \phi_1) + H\ \sin\ (\phi_2 - \beta) + K\ \sin(\phi_2)\cos(\phi_2) = 0 \tag{6}$$

In addition, the smallest eigenvalue λ_{min} of the Hessian matrix, the Jacobi matrix of the derivatives of the energy Eq.(3), has to be positive.

3. PHASE DIAGRAM FOR $\beta = 0$

For $\beta = 0$ the external magnetic field is parallel to the direction of the easy axis. We find two ferromagnetic phases, $\mathbf{F}^{\uparrow\uparrow}$ and $\mathbf{F}^{\downarrow\downarrow}$ specified by the angles $\phi_1 = \phi_2 = 0$ and $\phi_1 = \phi_2 = \pi$, respectively. The corresponding energies are $E_F = 2 - 2H$ and $E_F = 2 + 2H$. The two ferromagnetic phases $\mathbf{F}^{\uparrow\uparrow}$ and $\mathbf{F}^{\downarrow\downarrow}$ are stable for $H > 4 - K$ and $H < K - 4$, respectively. We further find the anti-ferromagnetic phase **AF** characterized by the angles $\phi_1 = 0\ \phi_2 = \pi$, and $\phi_1 = \pi\ \phi_2 = 0$ with the corresponding constant energy $E_{AF} = -2$. The antiferromagnetic phases are stable for $|H| < \sqrt{K(4+K)}$. Eventually there exists a scissored phase SC specified by the angle relation $\phi_1 = -\phi_2$ with $\phi_1 = \mathrm{Arccos}H/(4-K)$. Note that his phase is often referred to as the spin-flop phase [7]. The corresponding energy takes the value $E_{SC} = (K-2) - H^2/(4-K)$.

This phase is stable for $|H| < 4 - K$ and $|H| > (4-K)\sqrt{K/(4+K)}$. Note that the scissored phase exists only for $K < 4$. According to Fig. 3 we can have coexistence of two and more phases, respectively. Moreover, we have the triple points $P_3 = (\frac{4}{3}, \pm\frac{8}{3})$, where three phases exist, while at $P_4 = (4, 0)$ we have coexistence of all four phases. These critical points will be decisive in order to give a proper classification of all possible hysteresis loops. The evolution of the two magnetization angles ϕ_1 and ϕ_2 as a function of the magnetic field for an anisotropy strength below the critical point $K = \frac{4}{3}$ is illustrated in Fig. 4.

We start with a sufficiently large positive field and drive the field slowly down. The first transition occurs, when the $F^{\uparrow\uparrow}$ phase becomes unstable. ($P_{F^{\uparrow\uparrow}\to SC} = (1, 3)$). This second order transition is a pitchfork bifurcation. Then the SC phase becomes unstable and there is a discontinuous transition at $P_{SC\to AF} = (1, \frac{3}{5}\sqrt{5})$. Then the AF phase becomes unstable and we reenter the SC phase at $P_{AF\to SC} = (1, -\sqrt{5})$. Eventually the SC phase becomes unstable at $P_{SC\to F^{\downarrow\downarrow}} = (1, -3)$ and we enter continuously the complementary ferromagnetic phase $F^{\downarrow\downarrow}$.

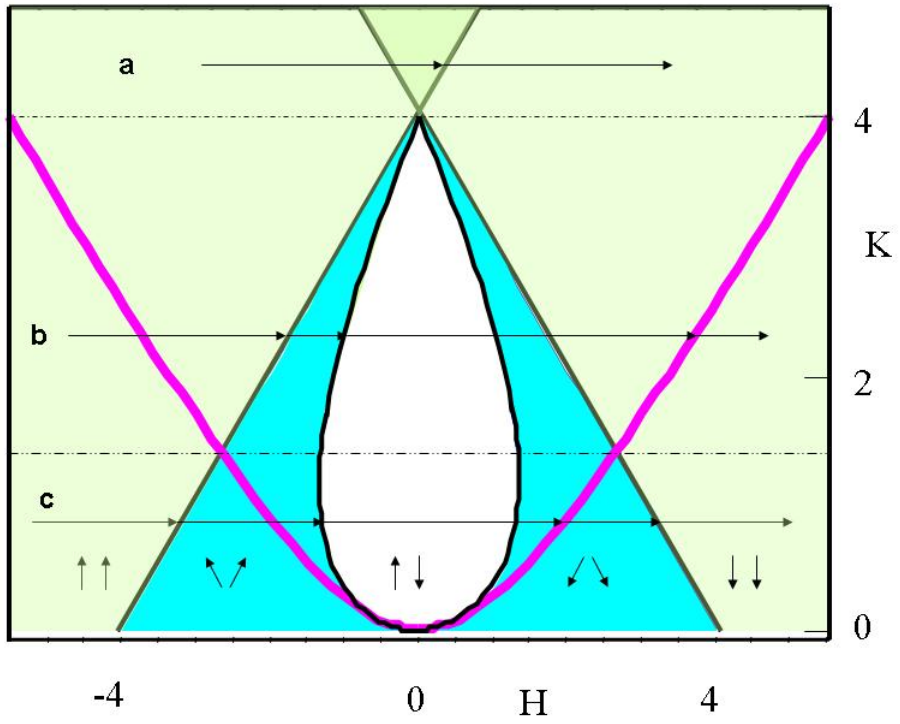

FIG. 5: A diagram of different states existing in a magnetic tunnel junction as a function of external magnetic field. The field is applied in the plane parallel to ferromagnetic layers and the shape of the particles is associated with the parameter K. Large positive value of K indicate that the monodomain particles are strongly elongated along X-direction.

In contrast to the evolution of the magnetization angles in Fig. 4 we restart with a negative large saturation and drive the field slowly up to the positive saturation again. Thus, in contrast to Fig. 4, Fig. 5 is symmetric to the axis of magnetization, since we drive the saturated field forth and back, giving rise to a closed hysteresis loop. The evolution of the two magnetization angles for anisotropy strength K with $\frac{4}{3} < K < 4$ between the two critical points is similar, however the system enters directly from the AF phase into the $\mathbf{F}^{\downarrow\downarrow}$ without passing through the **SC** phase. In fact, this behavior is well known from experiments with antiferromagnetic materials.

Figure 4 shows the corresponding evolution of the hysteresis loop, which can also be extracted completely from our phase diagram depicted in Fig. 3.

According to the phase diagram depicted in Fig. 3, for $K > 4$, we only have transitions from the ferromagnetic phase $F^{\uparrow\uparrow}$ to the complementary ferromagnetic $F^{\downarrow\downarrow}$ phase and vice versa.

We stress that a complete classification of all possible hysteresis curves is of fundamental importance in any kind of technical application. Moreover, in the same manner, the qualitative behaviour of all possible magnetoresistance curves can directly be extracted from the phase diagram depicted in Fig. 3.

4. Hysteresis Loops

Hysteresis loops are found that correspond directly to the previous phase diagram.

The orientation of the magnetisation is shown in Figures X, Y, and Z as the magnetic field is successively lowered and heightened through negative and positive values. The field is directed in parallel to the easy axes of the single domain particles. In Figure 3 there is a level of anisotropy, $K/J > 4$, where the phase transition between the ferromagnetically ordered states $\uparrow\uparrow$ and $\downarrow\downarrow$ is seen. For one such value of K in Figure 3 the phase transition is mapped out by the progression of linear arrows across the spectrum of H and is depicted by (a). In Figure X the curve with

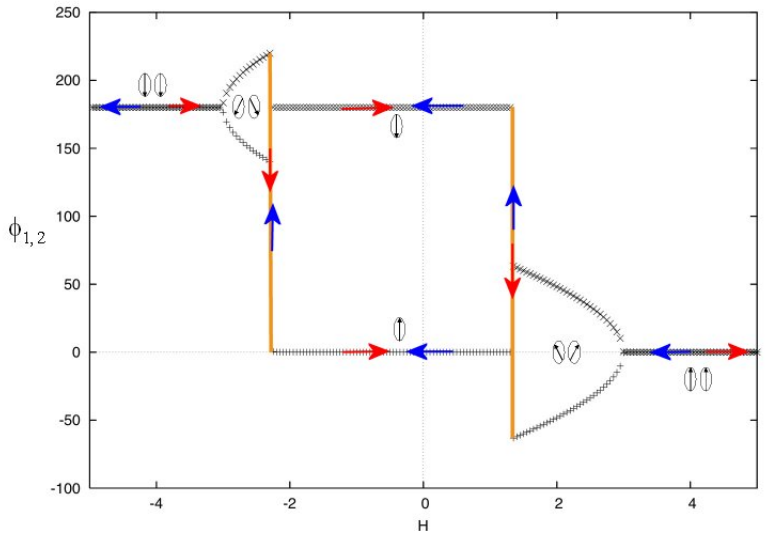

FIG. 6: The magnetisation angles of the two layers as a function of magnetic field and anisotropy parameter K=1

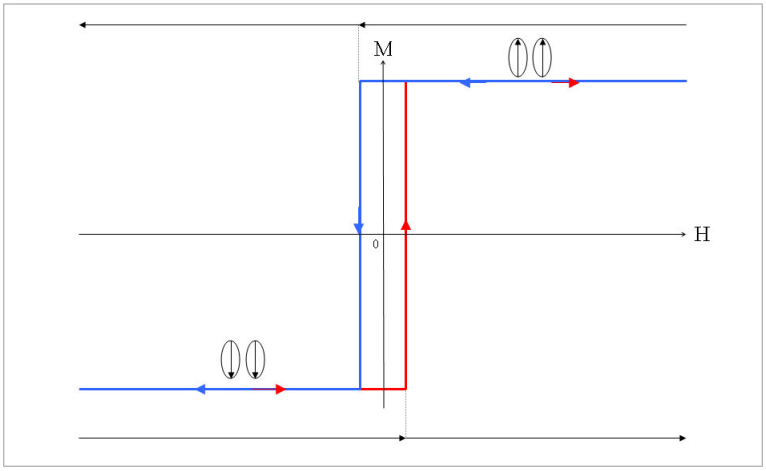

FIG. 7: Figure X The total magnetisation as a function of applied magnetic field strength. This hysteresis curve is illustrative of the process highlighted in Fig 3 at point "a". The arrows below the curve are those seen in Fig 3 at this point, marking the transition between the flipped states of the ferromagnetic alignments.

respect to (a) in Fig 3 is shown. As the value H increases positively the system remains in the ↓↓ orientation until a critical point where a jump is made to the ↑↑ state. Conversely, when the field is in turn lowered progressively the critical level is reached at a point which mirrors that of the preceding evolution and a jump is made from ↑↑ to ↓↓. At a level of K in Figure 3 there exists a more complicated phase distribution. For K at level (b) in the diagram there is the addition of scissor states, e.g. ↙↘, and antiferromagnetically ordered ones. Traversing the line along (b) the ferromagnetic ordering persists until a level of field where a scissors state begins to emerge. Going from the low negative field upwards, the condition of the magnetisation of one particle is found at an angle ϕ_1, whereas for the other it is the direct inverse. Taking ϕ_1 and ϕ_2 to be 180 degrees from zero in the case of the ferromagnetic state, the scissors state begins by splaying the magnetisation directions outward from an imaginary central axis. The splaying begins moderately but as the field comes from the low negative strength upwards the overall angle between the magnetisation vectors increases. This continues until a critical point where one particle aligns itself with the field

and the other becomes the very antithesis of the first. This point is marked by a jump up to zero magnetisation in Figure Y. Increasing the field out of the negative regime, through zero and up to a juncture in the magnetisation characteristics where the moments align themselves ferromagnetically upwards in the positive field, the final jump in the forward evolution is seen. This will happen when the field wins out against all other opposing factors and flips both particles under its influence and into its orientation. Beginning the reduction of the field reversed the process in a manner that gives a negative reflection of the magnetisation. The hysteresis curve in Figure Y is now attained.

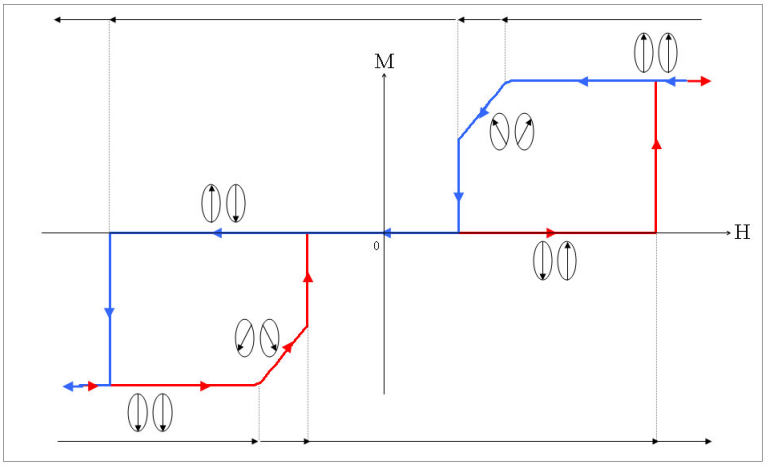

FIG. 8: Figure Y The total magnetisation as a function of applied magnetic field strength. This hysteresis curve is illustrative of the process highlighted in Fig 3 at point "b". The arrows below the curve are those seen in Fig 3 at this point, marking the transition between the differerent alignments.

With H equal to zero, and until a point in the field strength where anisotropy no longer holds sway, the system is in an artificial antiferromagnetically ordered state with a moderate level of anisotropy K. The final hysteresis curve described here, Figure Z, has the lowest level of uniaxial anisotropy and as such is the one with the smallest return loops and greatest propensity for its moments to fluctuate. Beginning with low negative field strength the system starts in its ferromagnetic alignment in harmony with the direction of the field. This saturated magnetisation state ends earlier than for higher values of K and a scissors state propagates. This state lasts over a greater range of the magnetic field in this softer material than in the other two hysteresis curves before jumping to the antiferromagnetic distribution. Antiferromagnetism between the particles is maintained until the jump to a new scissors state is made at another critical level of applied field strength. These new scissors begin to close as the field comes to dictate more until they become parallel and the complete flip of both particles has arrived. Upon reversing the magnetic fields cycle the hysteresis curve is born, showing smaller hysteresis and consequentially less energy loss than its predecessors. The material featuring in this kind of curve is one that has a more rapid response to the field and a small remanence. The particles magnetisations align opposite to one another with zero H due to the demagnetisation fields or rather the fields arising from the magnetic poles at the edges of the elliptical particles.

PHASE DIAGRAM FOR $\beta = \frac{\pi}{4}$

The necessary condition for the existence of a local minimum of the Hamiltonian is

$$-2\sin(\phi_1 - \phi_2) + H\ \cos\frac{\pi}{4}(\sin\ (\phi_1) - \cos(\phi_1)) + K\ \sin(\phi_1)\cos(\phi_1) = 0 \tag{1}$$

$$+2\sin(\phi_1 - \phi_2) + H\ \cos\frac{\pi}{4}(\sin\ (\phi_2) - \cos(\phi_2)) + K\ \sin(\phi_2)\cos(\phi_2) = 0 \tag{2}$$

Moreover at the critical lines the determinant of the Hessian

$$Det\left((\frac{\partial^2 H(\phi)}{\partial\phi_i\partial\phi_j})_{|\phi=\phi^*}\right) \tag{3}$$

has to be zero. We find the two ferromagnetic phases, $\mathbf{F}^{\uparrow\uparrow}$ and $\mathbf{F}^{\downarrow\downarrow}$ specified by the angles

$$\sin(\phi_1 - \frac{\pi}{4}) = -\frac{H}{2K}(\sqrt{1 + 2(\frac{K}{H})^2} - 1)$$

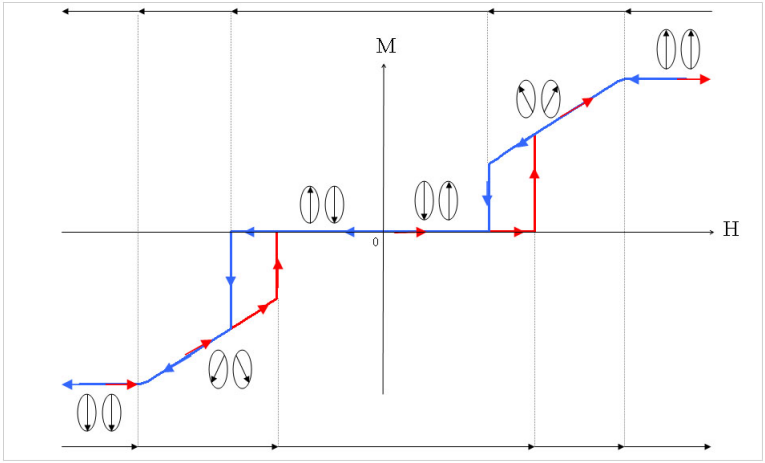

FIG. 9: Figure Z The total magnetisation as a function of applied magnetic field strength. This hysteresis curve is illustrative of the process highlighted in Fig 3 at point "c". The arrows below the curve are those seen in Fig 3 at this point, marking the transition between the magnetisation orientations

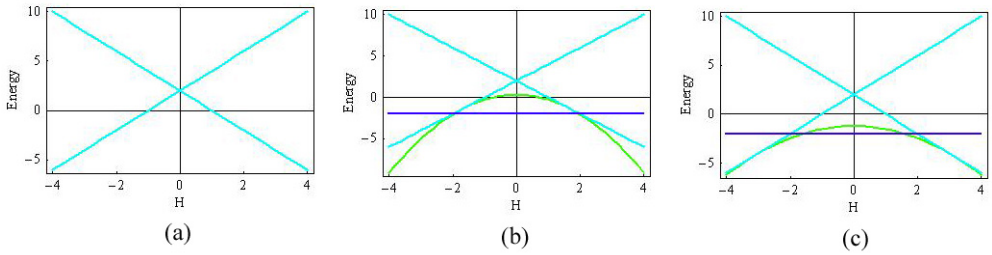

FIG. 10: Energies against magnetic field strength for (a) the evolution of "a"through figure 3, (b) the evolution of "b" through figure 3, (c) the evolution of "c" through figure 3. In (a) The energies correspond to the $\uparrow\uparrow$ state for the negative slope and $\downarrow\downarrow$ state for the positive slope. In (b) the zero slope line (blue online) corresponds to the antiferromagnetic orientations, whilst the parabola comes about due to the scissor states (green online). The energy dependence upon H in (c) is as in (b) except the anisotropy parameter is 0.8 as opposed to 2.3. This parameter is taken to be 4.3 in (a).

$\phi_2 = \phi_1$ for $H > -K/2$, while for $H < K/2$ ....(symmetry!). with $E_F =$ .... The lines of stability of the ferromagnetic phases are not analytic. They satisfy the nonlinear equation

$$4H^6 + H^4(15K^2 - 64) + 4H^2K^2(3K^2 - 16) - (4K^6 - 128K^4 + 1024K^2) = 0$$

In the large H- and K-limit the phase boundaries of the two ferromagnetic phase approach $K(H) = 2H$ and $K(H) = -2H$, respectively. Note that the transitions from $\mathbf{F}^{\uparrow\uparrow}$ and $\mathbf{F}^{\uparrow\uparrow}$ to the scissored phase are always first order transitions, where the two angles ϕ_1 and ϕ_2 change discontinously their magnetic directions. The phase diagram is depicted in Fig...

The scissored phase which is spread almost over the whole plane is nonanalytic, except at the cusp of its boundary. One finds $P_c(2\sqrt{2}, 2)$ with the two critical angles $\phi_1 = 0$ and $\phi_2 = \pi/2$, respectively. In contrast to the ferromagnetic transition this transition is of second order, where the two angles ϕ_1 and ϕ_2 undergo a backward bifurcation, when we increase the strength of the magnetic field H.

$K = \alpha H$ **critical line**

CASE $\beta = \frac{\pi}{4}$

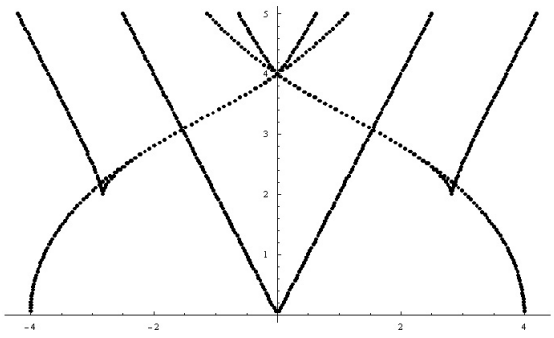

FIG. 11: Phase diagram as function of the magnetic field Hi for $\beta = \frac{\Pi}{4}$

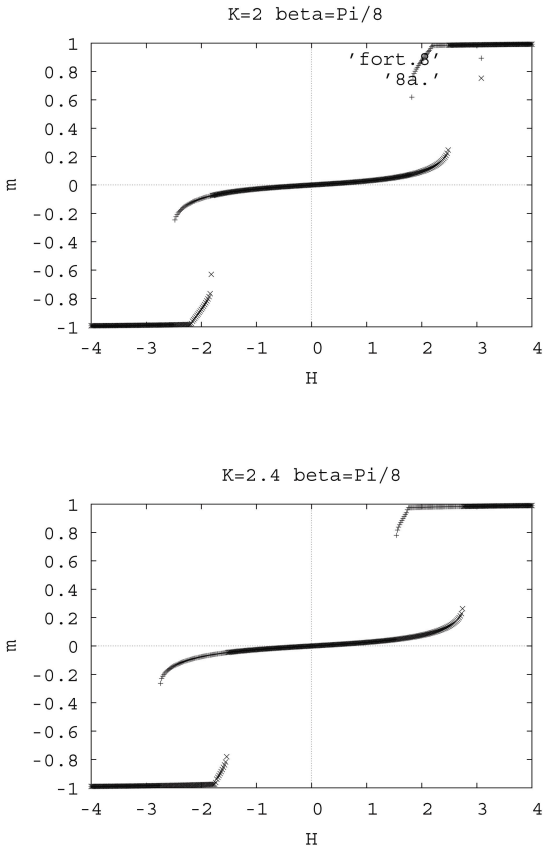

FIG. 12: Hysteresis loops for $\beta = \pi/8$ and K=2, and K=2.4

For $\beta = \frac{\pi}{4}$ we find $\alpha = 2$ (compare figure phase diagram) such that

$$K(H) = 2H$$

with the two angles $\phi_1 = \phi_2 = \frac{3\pi}{4}$. These two collinear angles do not depend on the field H. Note that here Eq.(1), Eq.(2), and Eq.(3) are simultaneously satisfied. Consequently, the point $P_c = (\frac{3\pi}{4}, \frac{3\pi}{4})$ represents a critical stationary point. (See figures below)

For $K = 2H$ and $\beta = \frac{\pi}{4}$ the variational force equilibrium equations Eq.(1) and Eq.(2) yield two additional collinear

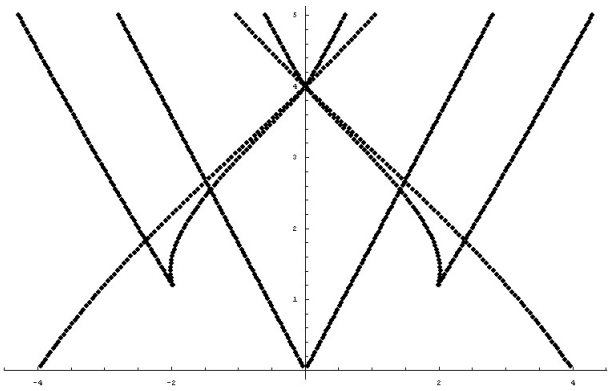

FIG. 13: Phase digram for $\beta = 22.5$

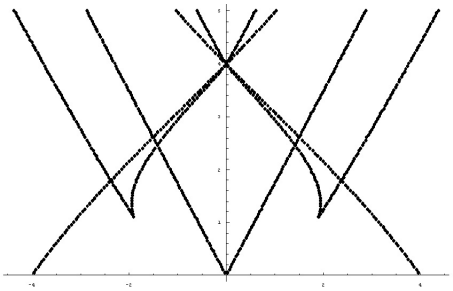

FIG. 14: Phase digram for $\beta = 20$

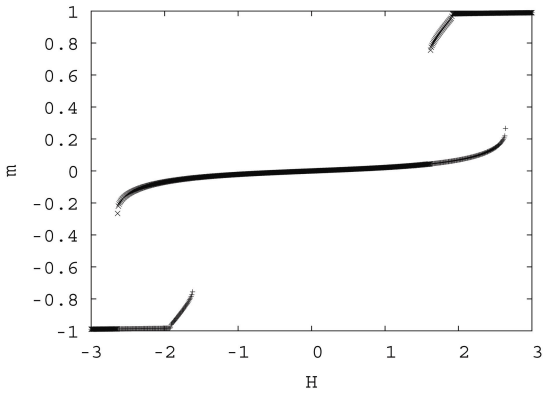

FIG. 15: Hysteresis loops for $\beta = 20$ and K=2.2

solutions (Eq.3 is not satisfied), namely

$$\phi = \frac{\pi}{12} \text{ and } \phi = \frac{17\pi}{12}$$

Also these two stationary points $P(\frac{\pi}{12}, \frac{\pi}{12})$ and $P(\frac{17\pi}{12}, \frac{17\pi}{12})$ do not depend on the field H. The corresponding eigenvalues of the Hessian signal a relative minimum and a relative maximum. The relative minimum can be shown to be stable only for $H \geq \frac{8}{\sqrt{27}}$. (As to be expected) the critical point lies exactly between the relative minimum $P_{min}(\frac{\pi}{12}, \frac{\pi}{12})$ and the relative maximum $P_{max}(\frac{17\pi}{12}, \frac{17\pi}{12})$

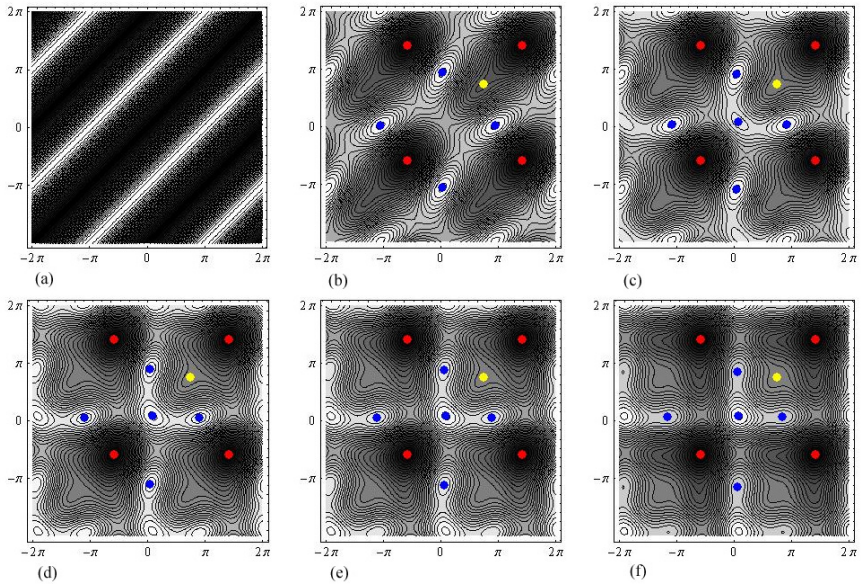

FIG. 16: Energy contours as a function of magnetic field, taken when $K = 2H$. The angles of the particles are on the x and y axes and the minima are depicted by blue dots, the maxima by red ones and the second order critical points by their yellow counterparts. (a) $H = 0$, (b) $H = 1$, (c) $H = 2$,(d) $H = 3$,(e) $H = 4$ and (f) $H = 10$

other analytic cases: $\beta = 0$ and $\beta = \frac{\pi}{12}$

For $\beta = 0$ we have $K(H) = H$ with the angles $\phi_1 = \phi_2 = \pi$

For $\beta = \frac{\pi}{12}$ we have $K(H) = 1.62...H$ with the angles $\phi_1 = \phi_2 = 2.57..$ $(\phi_i = \pi + ..)$ is also a solution!

The angles are the solutions of the nonlinear equation

$$\cos(\frac{\pi}{12} - \phi) + \sin(\frac{\pi}{12})\,(\cot(\phi) - \tan(\phi)) = 0$$

and for α we have

$$\alpha = \csc(\phi)\sec(\phi)\sin(\frac{\pi}{12} - \phi)$$

SUMMARY

We studied properties of two interacting magnetic particles subjected to exchange interaction J, anisotropy parameter K and an external magnetic field H with an arbitrary angle β with respect to the easy axis. We further present a complete theoretical study of magnetic phase diagrams as a function of the field for arbitrary strength of the anisotropy. We classify all possible magnetic hysteresis loops and show the dependence of the corresponding magnetic moments on the external field. These studies can give answers to the problem of finding adequate materials for practical applications such as sensor, storing or recording devices. We remark that for larger number of particles the problem of multistability is highly complex and can lead to fractal properties seen in all physical variables [8].

In conclusion, we have demonstrated the behavior of MTJ consisting of pair of diskshape monodomain particles separating by an insulator. We have studied the stability of the MTJ states and a hysteresis loop both analytically and numerically and made a detailed analysis of the possible hysteresys loops of the proposed MTJ. We have determined a phase diagramm in the magnetic field -shape anisotropy plane. The numerical calculations are in good agreement with our theoretical predictions.

The proposed MTJ may entail a range of applications. Development of new magnetoelectronic devices are probable and innovations in information processing and THz technology can be anticipated. The possible applications may include models for MRAM constructions and logic gates. The novel magnetoelecronic devices may embrace memory cells for storing binary data and even a construction for logic gates. Many interconnected transmission lines made of MTJ can be designed into networks – nano MTJ networks. These considerations lead to future development of a novel hardware and a new technology based on the nano- MTJs.

ACKNOWLEDGMENTS

This work has been supported by the European Science Foundation (ESF) in the framework of the network program: "Arrays of Quantum Dots and Josephson Junctions".

[1] M. A. Howson, *Contemporary Physics*, **35**, (5) 347-359 (1994)

[2] P. Grünberg, *Physics Today*, May 2001

[3] R. P. Cowburn and M. E. Welland, Science, **287**, 1466 (2000)

[4] D. Suess, T. Schrefl, W. Scholz, and J. Fidler, Journal of Magnetism and Magnetic Materials, **242-245**,426-429 (2002)

[5] D. C. Worledge, Appl. Phys. Lett. **84**, 2847 (2004)

[6] Z. Szabo and A. Ivanyi, Journal of Magnetism and Magnetic Materials, **215-216**, 33-36 (2000)

[7] C Micheletti, R.B. Griffiths and J.M. Yeomans, Phys.Rev. **B 59**, 6239 (1999)

[8] K. E. Kürten and F.V Kusmartsev, Phys.Rev. **B 72**, 014433 (2005)

[9] Daughton, J.; Magnetoresistive Random Access Memory; 2000.

[10] Klein, L.; Single-layer PHE-based MRAM; 2005.

[11] Akerman, J.; Toward a Universal Memory; Science; 308(4), 508-510; 2005.

[12] Mallinson, John; Magneto-Resistive and Spin Valve Heads; Academic Press; 2002.

[13] Hirota E., Sakakima H., Inomata K,; Giant Magneto-Resistance Devices; Springer; 2002.

[14] Hartmann, Uwe (editor); Magnetic Multilayers and Giant Magnetoresistance; Springer; 2000.

[15] Daughton, James M, Advanced MRAM Concepts; NVE Corporation, 2001.

[16] Slaughter J.M et al; Fundamentals of MRAM Technology; Journal of Superconductivity; 15(1), 19; 2002.

[17] Daughton, J.M.; J. Appl. Phys; 81(8), 3758.

[18] Durlam, M et al.; VLSI Symposium 2002.

[19] Durlam, M., et al.; A 0.18um 4Mb Toggling MRAM; Freescale Semiconductor, Inc.; 2003.

[20] Pohm, A.V. et al.; IEEE Transactions on Magnetics; 33(5), 3280.

[21] Slaughter, J.M., et al.; Magnetic Tunnel Junction Materials for Electronic Applications; JOM-e, 52(6); 2000: